β-D-Xylosidase from *Selenomonas ruminantium*: Role of Glutamate 186 in Catalysis Revealed by Site-Directed Mutagenesis, Alternate Substrates, and Active-Site Inhibitor

Douglas Brian Jordan · Jay D. Braker

Abstract β-D-Xylosidase/α-L-arabinofuranosidase from *Selenomonas ruminantium* is the most active enzyme known for catalyzing hydrolysis of 1,4-β-D-xylooligosaccharides to D-xylose. Catalysis and inhibitor binding by the GH43 β-xylosidase are governed by the protonation states of catalytic base (D14, pK_a 5.0) and catalytic acid (E186, pK_a 7.2). Biphasic inhibition by triethanolamine of E186A preparations reveals minor contamination by wild-type-like enzyme, the contaminant likely originating from translational misreading. Titration of E186A preparations with triethanolamine allows resolution of binding and kinetic parameters of the E186A mutant from those of the contaminant. The E186A mutation abolishes the pK_a assigned to E186; mutant enzyme binds only the neutral aminoalcohol $\left(\text{pH} - \text{independent } K_i^{\text{triethanolamine}} = 19\,\text{mM}\right)$, whereas wild-type enzyme binds only the cationic aminoalcohol $\left(\text{pH} - \text{independent } K_i^{\text{triethanolamine}} = 0.065\,\text{mM}\right)$. At pH 7.0 and 25°C, relative kinetic parameter, $k_{\text{cat}}^{\text{4NPX}}/k_{\text{cat}}^{\text{4NPA}}$, for substrates 4-nitrophenyl-β-D-xylopyranoside (4NPX) and 4-nitrophenyl-α-L-arabinofuranoside (4NPA) of E186A is 100-fold that of wild-type enzyme, consistent with the view that, on the enzyme, protonation is of greater importance to the transition state of 4NPA whereas ring deformation dominates the transition state of 4NPX.

Keywords Fuel ethanol · Glycoside hydrolase · GH43 · pH dependence · Relative substrate specificity

D. B. Jordan (✉) · J. D. Braker
Fermentation Biotechnology Research Unit, National Center for Agricultural Utilization Research, Agricultural Research Service, U.S. Department of Agriculture, 1815 N. University Street, Peoria, IL 61604, USA
e-mail: douglas.jordan@ars.usda.gov

Introduction

β-D-Xylosidase/α-L-arabinofuranosidase of the ruminal, anaerobic, and nonxylanolytic bacterium *Selenomonas ruminantium* (SXA) belongs to glycoside hydrolase family 43 (GH43) and structural clan F of the CAZy database (carbohydrate active enzymes database, http://www.cazy.org/) [1–3]. The enzyme is the most potent catalyst known, to date, for promoting the hydrolysis of 1,4-β-D-xylooligosaccharides to D-xylose. Its k_{cat} and k_{cat}/K_m are at least tenfold greater than those reported for other β-xylosidases [4, 5] when acting on oligoxylosides of increasing degrees of polymerization from xylobiose to xylohexaose. Catalytic prowess [4, 5], good stability versus challenges of denaturation by pH (stable above pH 4.0) and temperature (stable below 50°C) [6], and high level of protein production in *Escherichia coli* (approximately 30% of soluble cell protein as SXA with greater than 5 g SXA produced per liter of culture under nonoptimized conditions) [7] favor application of SXA in industrial processes where it would serve in the hydrolysis of herbaceous biomass (xylan fraction) to simple sugars for fermentation to fuel ethanol and other bioproducts [8–10].

In addition to its β-xylosidase activity (EC 3.2.1.37) on natural (xylooligosaccharides, arabinoxylan, and uronoxylan) and artificial substrates (4-nitrophenyl-β-D-xylopyranoside, 4NPX), SXA possesses α-arabinofuranosidase activity (EC 3.2.1.55) on natural (arabinoxylan) and artificial (4-nitrophenyl-α-L-arabinofuranoside, 4NPA) substrates [4, 11–15]. The arabinofuranosidase and xylosidase activities share the same active site of SXA, which, being composed of two subsites [12, 14, 16], constitutes the simplest possible active site available for catalytically efficient glycoside hydrolases. Because the α-L-arabinofuranose ring of 4NPA overlays well with the β-D-xylopyranose ring of 4NPX, bifunctionality of SXA for these substrates seems obvious (Scheme 1a) [11]. It has been determined that, off the enzyme and extrapolated to 25°C, the spontaneous rate of hydrolysis (at pH 5.3 in the pH-independent region) of 4NPA to L-arabinose and 4-nitrophenol is approximately 16-fold faster than that of 4NPX to D-xylose and 4-nitrophenol [15], and this is ascribed to the additional energy required for achieving coplanarity of C1, C2, C5, and O5 of the xylopyranose glycone from its chair configurations in the ground state in comparison to that of the arabinofuranose glycone, in proceeding from its ground states to coplanar configurations of C1, C2, C4, and O4 (10 versus 3–4 kcal/mol) [17]. On the enzyme at 25°C, rates of hydrolysis of 4NPX (pH-independent values for k_{cat} of 32.7 s^{-1} and k_{cat}/K_m of 58.7 s^{-1}mM^{-1} [4, 11]) and 4NPA (pH-independent values for k_{cat} of 3.25 s^{-1} and k_{cat}/K_m of 5.10 s^{-1}mM^{-1} [4, 11]) have the opposite order, and it seems evident that the catalytic machinery of SXA has been developed to act effectively in distorting the D-xylose ring to its transition-state configuration.

It has been established that SXA-catalyzed reactions proceed through an inversion mechanism, in which the stereochemistry of the anomeric carbon is inverted, with the concurrent action of the catalytic base (side chain carboxylate of D14, pK_a 5) serving to activate water for addition to C1 of the glycone moiety of substrate and the catalytic acid (side chain carboxylic acid of E186, pK_a 7) serving to protonate the aglycone leaving group to form the alcohol in the single transition state (Scheme 1b) [4]. There is only one other residue in the active site with a carboxyl group (D127), and it is not in position to satisfy either the role of catalytic acid or the catalytic base. Furthermore, comparison of the X-ray structure of the active site of SXA in complex with inhibitor Bis-Tris-propane with the X-ray structures of other GH43 β-xylosidase active sites (either ligand free or in complex with β-xylobiose) indicates very similar positions of active site residues and no apparent changes in conformation [14].
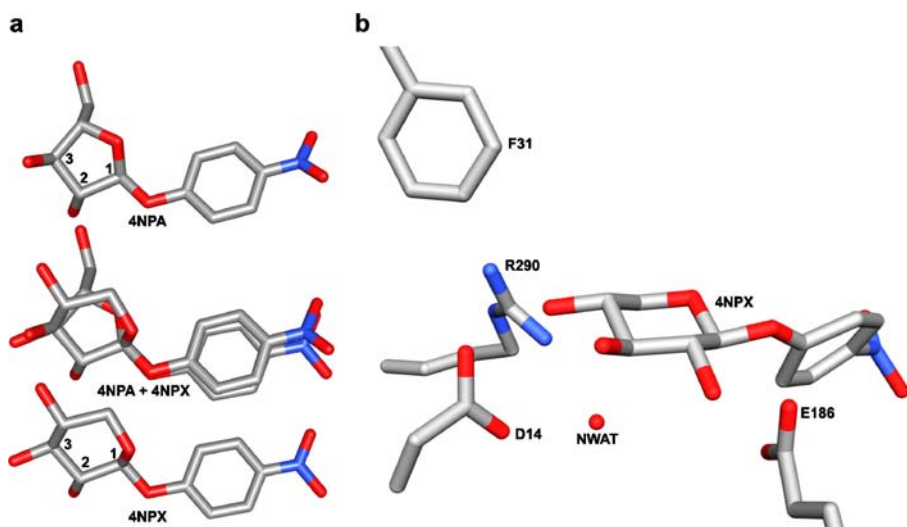
Scheme 1 Molecules discussed in the text. **a** 4NPA, overlay of 4NPA and 4NPX, and 4NPX. Atom numbering is indicated. **b** 4NPX in the active site. 4NPX was docked into the active site of the X-ray structure of SXA (PDG accession code, 3C2U) as described [14]. SXA active-site residues discussed are shown. *NWAT* nucleophilic water

Previous work revealed that certain site-directed mutations (F31A, R290A) within subsite −1, in which the catalytic base and catalytic acid reside, effect lower ratios of kinetic parameters, $k_{cat}^{4NPX}/k_{cat}^{4NPA}$, for the enzyme variants acting on 4NPX and 4NPA than the $k_{cat}^{4NPX}/k_{cat}^{4NPA}$ value determined for the wild-type SXA, indicating that the native residues are more important for facilitating 4NPX hydrolysis than 4NPA hydrolysis. The native residues have been assigned roles in promoting distortion of the D-xylose ring to its transition state configuration by acting on C4 of the xylosyl glycone (Scheme 1b) [11]. The same study reports that, although the individual kinetic parameters are much lower than those of wild-type SXA, the ratio $k_{cat}^{4NPX}/k_{cat}^{4NPA}$ for the E186A mutant is similar to that of the wild-type enzyme, suggesting that the catalytic acid exerts equal influences on the two transition states. Since then, when using the aminoalcohol, triethanolamine, to probe SXA active sites, we found that all E186A preparations (including one prepared with a His$_6$ appendage and purified with affinity chromatography for the His tag and one prepared in *E. coli* with its native, genomic β-xylosidase knocked out) show biphasic Dixon plots with respect to inhibition by competitive inhibitor, triethanolamine, with greater than 1,000-fold difference in affinity for triethanolamine between the two enzyme species present in the E186A preparations [16]. The high affinity species (enzyme 1) is wild-type-like in its $K_{i(triethanolamine)}$ (0.1 mM at pH 7.0 and 25°C). Equilibrium binding studies of triethanolamine and E186A indicate that the low-affinity species (enzyme 2) dominates the protein content of E186A preparations. If the wild-type-like enzyme were wild-type SXA in its catalytic properties, it would constitute less than 0.03% of the protein in the E186A preparations. Thus, the wild-type-like enzyme activity is seen as a contaminant that likely arises through translational misreading [16].

With the triethanolamine method established [16], for the work reported here, we set out to resolve the kinetic parameters of the E186A mutant acting on 4NPX and 4NPA from those of the wild-type like contaminant. We report a much larger value of $k_{cat}^{4NPX}/k_{cat}^{4NPA}$

determined for the E186A mutant (enzyme 2, low affinity for triethanolamine) than that of
wild-type SXA, consistent with the view that the native E186, in its role as catalytic acid,
contributes little, if any, to the inversion of substrate conformation, making E186 more
important for promoting hydrolysis of 4NPA than 4NPX. Also, we separate the activities of
enzymes 1 and 2 to provide pH dependencies of kinetic parameters for the E186A mutant
acting on 4NPX. The successful approach provides information that allows us to assess the
roles of E186 in catalysis of 4NPA and 4NPX hydrolysis. Furthermore, it demonstrates
application of another useful method that can be applied to study other glycoside hydrolases
with regard to substrate distortion.

Materials and Methods

Materials and General Methods

Buffers, 4-nitrophenol (4NP), 4-nitrophenyl-β-D-xylopyranoside (4NPX), 4-nitrophenyl-α-L-
arabinofuranoside (4NPA), and triethanolamine (TEA) were obtained from Sigma-Aldrich (St.
Louis, MO, USA). 4NPA and 4NPX were also from Carbosynth (Bershire, UK). Water was
purified through a Milli-Q unit (Millipore; Billerica, MA, USA). All other reagents were
reagent grade and high purity. A Cary 50 Bio UV-Visible spectrophotometer (Varian; Palo
Alto, CA, USA), equipped with a thermostatted holder for cuvettes, was used for spectral and
kinetic determinations. An AVIV Model 215 circular dichroism spectrophotometer (Aviv
Biomedical; Lakewood, NJ, USA), equipped with thermostatted cuvette holder, and 1 mm
path-length quartz cuvettes was used for acquiring protein spectra; three spectra were averaged
for each protein sample. Molecular graphics were produced as described [11, 14] using the
coordinates of SXA in complex with Bis-Tris-propane (PDB accession code, 3C2U).

The gene encoding β-xylosidase from *S. ruminantium* GA192 was cloned and expressed
in *E. coli* [13]. E186A-SXA was prepared as described [4]. The E186G mutation of SXA was
introduced into the gene encoding for SXA within pET21(+) by using the QuikChange Site-
Directed Mutagenesis Kit (Stratagene; La Jolla, CA, USA) and the primers, 5′-cgatattgccta
taccggaggtccccacctttac-3′ and 5′-gtaaaggtggggacctccggtataggcaatatcg-3′ where the underlined
nucleotides indicate the mutations incorporated. The gene was fully sequenced, as described
[4], to confirm that only the intended mutations had been introduced. After transformation
into *E. coli* BL21(DE3), cells were grown and induced as described for the wt-SXA [4].
SXA, E186A-SXA, and E186G-SXA, produced in *E. coli*, were purified to homogeneity, as
judged by SDS-PAGE analysis [6], by using reverse phase and anionic exchange
chromatography steps as described [4] with the addition of a final desalting, gel filtration
step into 10 or 20 mM sodium phosphate, pH 7.3 as before [5, 11, 12, 14–16]. Circular
dichroism spectra (190–260 nm, collected for samples containing 8 μM enzyme in 20 mM
sodium phosphate, pH 7.3) are characterized by a major trough at 214 nm. The E186A and
E186G spectra are qualitatively similar to the wild-type SXA. Mean trough values $[[\theta]]$ at
214 nm: wild-type SXA $= (-3.32 \pm 0.04) \times 10^6$ deg•cm^2•$dmol^{-1}$, E186G mutant $=
-4.53 \pm 0.05 \times 10^6$ deg•cm^2•$dmol^{-1}$, and E186A mutant $= -3.00 \pm 0.07 \times 10^6$ deg•
cm^2•$dmol^{-1}$.

Reactions Catalyzed by E186A and E186G

All reactions (1 mL) were at the constant ionic strength (I=0.3 M, adjusted with sodium
chloride) at 25°C in the following pH buffers: 100 mM sodium succinate (pH 6.0), 100 mM

sodium phosphate (pH 7.0), and 30 mM sodium pyrophosphate (pH 8.0, 8.5, 9.0, and10.0). 4NPA and 4NPX concentrations varied from 0.05 to 7 mM. For each reaction condition, the indicated concentration of triethanolamine was included in the buffers for pH adjustment and its concentration was included in the ionic strength calculation. Thus, pH and ionic strength values of reaction mixtures are as indicated in the text. Initial rate data were collected by two methods. In method A, reactions, in 1 cm path-length cuvettes, were initiated by addition of enzyme (10–50 µL in 10 mM sodium phosphate, pH 7.3, at 25°C) and monitored continuously at 400 nm for 10–40 min. Rates were linear. 4NPA and 4NPX concentrations and delta extinction coefficients at 400 nm (product–substrate) for each reaction condition were determined as described [4]. The concentration of 4NP used for these determinations was calculated by using the reported extinction coefficient of 18.3 $mM^{-1} cm^{-1}$ at 400 nm for 4NP in NaOH [18]. In method B, after initiating reactions (time=0.3 min to 20 h) with enzyme (10–50 µL in 10 mM sodium phosphate, pH 7.3, at 25°C), 100 µL aliquots of reaction mixtures were removed and added to 1 cm path-length cuvettes containing 0.9 mL 0.1 M NaOH (for 4NPX reactions) or 0.9 mL 0.1 M sodium carbonate at pH 11 (for 4NPA reactions) and the absorbance was read at 400 nm. Absorbance versus time points (n=3–6) produced straight lines. The slopes were converted to molar changes using the extinction coefficient 18.3 $cm^{-1} mM^{-1}$. Both methods report initial rates of enzyme reactions (v) in units of s^{-1}, which is the molar product produced per second per molar enzyme protomer (active sites), the latter value calculated using the extinction coefficient at 280 nm of 129,600 $M^{-1} cm^{-1}$ [19].

Equations

Data were fitted to equations using the computer program Grafit (Erithacus Software) [20]. Simple weighting (constant error) was used for fitting most data; proportional error weighting was used to fit some data (e.g., pH curves). Symbol definitions are the following: v is the observed initial (steady-state) rate of catalysis, k_{cat} is the maximum rate of catalysis, S is the substrate concentration, K_m is the Michaelis constant, I is the inhibitor concentration, K_i is the dissociation constant for I from EI, v_{enz1} is initial (steady-state) rate of catalysis for enzyme 1, v_{enz2} is initial (steady-state) rate of catalysis for enzyme 2, $K_{i(enz1)app}$ is the uncorrected (for S and K_m) dissociation constant of I from EI (enzyme 1), $K_{i(enz2)app}$ is the uncorrected (for S and K_m) dissociation constant of I from EI (enzyme 2), $k_{cat(enz1)}$ is the maximum rate of catalysis (enzyme 1); $k_{cat(enz2)}$ is the maximum rate of catalysis (enzyme 2), $K_{m(enz1)}$ is the Michaelis constant (enzyme 1), $K_{m(enz2)}$ is the Michaelis constant (enzyme 2), $K_{i(enz1)}$ is the dissociation constant of I from EI (enzyme 1), $K_{i(enz2)}$ is the dissociation constant of I from EI (enzyme 2), p is the determined parameter at a single pH, P is the pH-independent value of the parameter, K_a is the acid dissociation constant of the group affecting P, H^+ is the proton concentration, K_{a1} is the acid dissociation constant of the first group affecting P, K_{a2} is the acid dissociation constant of the second group affecting P, P_1 is the first limit of p (associated with K_{a1}), and P_2 is the second limit of p (associated with K_{a2}), $K_{a(enz)}$ is the acid dissociation constant of the enzyme group affecting P, and $K_{a(inh)}$ is the acid dissociation constant of the inhibitor group affecting P.

$$v = \frac{k_{cat} * S}{K_m + S} \qquad (1)$$

$$v = \frac{k_{cat} * S}{K_m \left(1 + \frac{I}{K_i}\right) + S} \qquad (2)$$

$$v_{obs} = \frac{v_{enz1}}{1 + \frac{I}{K_{i(enz1)app}}} + \frac{v_{enz2}}{1 + \frac{I}{K_{i(enz2)app}}} \tag{3}$$

$$v_{obs} = \frac{k_{cat(enz1)} * S}{K_{m(enz1)}\left(1 + \frac{I}{K_{i(enz1)}}\right) + S} + \frac{k_{cat(enz2)} * S}{K_{m(enz2)}\left(1 + \frac{I}{K_{i(enz2)}}\right) + S} \tag{4}$$

$$K_{i(app)} = K_i(1 + S/K_m) \tag{5}$$

$$p = \frac{P}{1 + \frac{H^+}{K_a}} \tag{6}$$

$$p = \frac{P}{1 + \frac{H^+}{K_{a1}} + \frac{K_{a2}}{H^+}} \tag{7}$$

$$p = \frac{P_1}{1 + \frac{H^+}{K_{a1}}} + \frac{P_2 - P_1}{1 + \frac{H^+}{K_{a2}}} \tag{8}$$

$$p = \frac{P}{\left(1 + \frac{H^+}{K_{a(enz)}}\right) * \left(1 + \frac{K_{a(inh)}}{H^+}\right)} \tag{9}$$

Results and Discussion

Three methods were employed to determine kinetic parameters and triethanolamine binding constants $\left(K_i^{TEA}\right)$ for the two β-xylosidase components of E186A preparations (Fig. 1a–c). Dixon plots, such as that of Fig. 1a, illustrate the biphasic inhibition profile of E186A preparations seen with active-site inhibitor, triethanolamine. The kinetic data fit well to Eq. 3, which describes inhibition of two enzymes (enzymes 1 and 2), with very different apparent K_i values, acting on a single concentration of substrate in the absence and presence of varied inhibitor concentrations. The reactions, conducted at pH 7.0 and 25°C, contained 51 μM 4NPX, which is 0.116-fold and 0.016-fold that of the K_m^{4NPX} values held by enzyme 1 (high affinity for triethanolamine, wild-type SXA-like affinity) and enzyme 2 (low affinity for triethanolamine, attributed to E186A variant of SXA), respectively. Corrections of the determined apparent K_i^{TEA} values for substrate concentration to arrive at true K_i^{TEA} values are minor and obtained by dividing the apparent value by the term, $(1+S/K_m)$, which is 1.116 for enzyme 1 and 1.016 for enzyme 2 at pH 7.0 and 25°C: thus, for the data of Fig. 1a, K_i^{TEA} values are 0.114±0.003 and 147±8 mM, respectively, for enzymes 1 and 2. Also, because of the low substrate concentration, values of k_{cat}/K_m for the two enzymes are

nearly equal to v/S and can be explicitly obtained by multiplying the individual velocities by the term, $(1/S + 1/K_m)$, or 21.9 for enzyme 1 and 19.9 for enzyme 2: thus, $k_{cat}/K_{m(enz1)}^{4NPX}$ is $(2.78 \pm 0.02) \times 10^{-3} \, s^{-1} \, mM^{-1}$ for enzyme 1 and $(0.635 \pm 0.008) \times 10^{-3} \, s^{-1} \, mM^{-1}$ for enzyme 2. The K_i^{TEA} value determined for enzyme 1 (0.114 mM) at pH 7.0 and 25°C is similar to that of wild-type SXA (0.111 ± 0.002 mM) [16], whereas that of enzyme 2 is 1,200-fold larger. The method of Fig. 1a was used throughout the pH range studied (pH 6–10).

The second method, shown as the double reciprocal plot of Fig. 1b, varies substrate and inhibitor where the lowest inhibitor concentration is enough to inhibit enzyme 1 catalytic activity to insignificant levels. Thus, kinetic parameters for enzyme 2 are determined by fitting the kinetic data to Eq. 2; kinetic parameters for enzyme 1 are not determined. The third method is the preferred method of the three, but it could not be used to determine kinetic parameters for enzyme 1 at pH 9 and 10 because of the low activity of enzyme 1 at high pH (pK_a of wt-SXA is 7.0). Figure 1c shows that, in this method, substrate and inhibitor are varied and the data are fitted globally to Eq. 4. Values for all kinetic parameters and binding constants are provided through the fit. Inspection of the quality of the data can be made by fitting individual curves of Fig. 1c to Eq. 3 (e.g., as was done for Fig. 1a) followed by making secondary plots as shown in Fig. 1d, e. Figure 1d shows v_{enz1} and v_{enz2} values, obtained by fitting individual curves of Fig. 1c to Eq. 3, plotted versus [4NPX]. Fitting the curves of Fig. 1d to Eq. 1 provides K_m and k_{cat} values similar to those obtained from the global fit to Eq. 4 of Fig. 1c. Figure 1e shows the $1/K_{i(app)}^{TEA}$, obtained by fitting individual curves of Fig. 1c to Eq. 3, plotted versus [4NPX]. Fitting the curves of Fig. 1e to Eq. 5 provides K_i^{TEA} values, similar to those obtained from the global fit of Fig. 1c data to Eq. 4.

Similar to our observations of v_{enz1}, v_{enz2}, $K_{i(enz1)}^{TEA}$, and $K_{i(enz2)}^{TEA}$ in a previous study [16], in the present study we find that whereas the values for v_{enz2}, $k_{cat(enz2)}$, $K_{i(enz1)}^{TEA}$, and $K_{i(enz2)}^{TEA}$, determined under identical conditions, were consistent between preparations, v_{enz1} and $k_{cat(enz1)}$ varied from preparation to preparation of E186A. For example, from reactions at pH 7.0, 25°C, and 51 μM 4NPX, determined values for preparations 1 and 4, respectively, are the following: v_{enz2}, $(3.19 \pm 0.04) \times 10^{-5} \, s^{-1}$ and $(3.02 \pm 0.32) \times 10^{-5} \, s^{-1}$; $K_{i(enz1)}^{TEA}$, 0.114 ± 0.003 and 0.142 ± 0.004 mM; $K_{i(enz2)}^{TEA}$, 147 ± 8 and 110 ± 42 mM, and v_{enz1} is $(1.27 \pm 0.01) \times 10^{-4} \, s^{-1}$ and $(5.80 \pm 0.05) \times 10^{-4} \, s^{-1}$. Also, global fits of data obtained at pH 6.0 and 25°C with varied 4NPX and TEA can be compared between that of Fig. 1c (preparation 5) and that of Table 1 (preparation 7). The following parameter values were determined for preparation 5: $k_{cat(enz1)} = (2.60 \pm 0.14) \times 10^{-2} \, s^{-1}$, $k_{cat(enz2)} = (1.45 \pm 0.07) \times 10^{-3} \, s^{-1}$, $k_{cat}/K_{m(enz1)} = (1.34 \pm 0.06) \times 10^{-2} \, s^{-1} \, mM^{-1}$, $k_{cat}/K_{m(enz2)} = (5.30 \pm 0.33) \times 10^{-4} \, s^{-1} \, mM^{-1}$, $K_{m(enz1)} = 1.94 \pm 0.18$ mM, $K_{m(enz2)} = 2.73 \pm 0.21$ mM, $K_{i(enz1)} = 0.671 \pm 0.036$ mM, and $K_{i(enz2)} = 506 \pm 133$ mM. The following parameter values were determined for preparation 7: $k_{cat(enz1)} = (4.51 \pm 0.07) \times 10^{-3} \, s^{-1}$, $k_{cat(enz2)} = (1.44 \pm 0.03) \times 10^{-3} \, s^{-1}$, $k_{cat}/K_{m(enz1)} = (1.43 \pm 0.03) \times 10^{-3} \, s^{-1} \, mM^{-1}$, $k_{cat}/K_{m(enz2)} = (5.10 \pm 0.15) \times 10^{-4} \, s^{-1} \, mM^{-1}$, $K_{m(enz1)} = 3.15 \pm 0.11$ mM, $K_{m(enz2)} = 2.82 \pm 0.12$ mM, $K_{i(enz1)} = 0.592 \pm 0.018$ mM, and $K_{i(enz2)} = 418 \pm 58$ mM. Clearly, parameters with v_{enz1} and $k_{cat(enz1)}$ terms are not similar between preparations, whereas the remaining parameters are quite similar, which is consistent with translational misreading as the cause of the minor contaminant of all E186A preparations. Whether the growth habit of *E. coli* cells or other factors change the quantity of enzyme 1 produced in the preparations has not been investigated. Therefore, limited kinetic information on enzyme 1 of E186A preparations, an enzyme with some wild-type properties and unknown amino acid sequence, can be obtained from the experiments reported here, whereas full steady-state kinetic parameters on enzyme 2, the true E186A mutant, can be obtained. It should also be noted that, particularly at lower pH, the K_i^{TEA} values are not
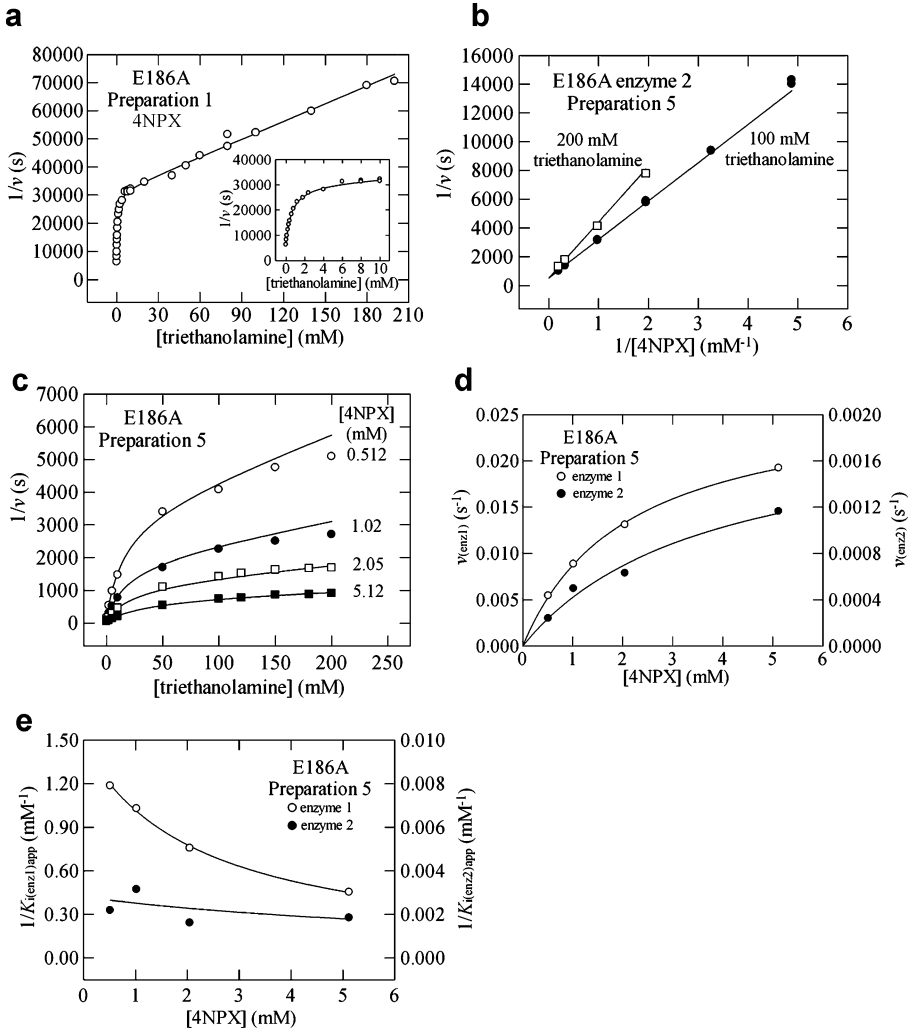
precisely determined for enzyme 2 because the upper triethanolamine concentrations were limited by the ionic strength (I=0.3 M) of the reactions. For example, at pH 6.0, whereas the $K_{i(enz1)}^{TEA}$ values are well determined with the enzyme 1 (high TEA affinity) of preparation 7 acting on 4NPA and 4NPX, the $K_{i(enz2)}^{TEA}$ value of enzyme 2 (low TEA affinity) of preparation 7 acting on 4NPX has a larger standard error (Table 1). This owes to the highest concentration of triethanolamine in the reactions being less than half of the determined inhibition constant for enzyme 2, so the greatest percent inhibition by triethanolamine was 20% in reactions. The $K_{i(enz2)}^{TEA}$ value of enzyme 2, preparation 7 acting on 4NPA is not determined (10^{23} mM; Table 1). This owes to the relatively low concentration of triethanol- amine that could be used (as with 4NPX reactions) and the much lower catalytic activity of enzyme 2 acting on 4NPA than 4NPX. The imprecise or undetermined $K_{i(enz2)}^{TEA}$ values are unimportant for good separation of kinetic parameters (enzyme 1 from enzyme 2) and simply indicate that enzyme 2 is weakly inhibited by triethanolamine, the basis of the resolution of

Fig. 1 Resolution of kinetic parameters of β-xylosidase components of E186A preparations by selective inhibition with triethanolamine. **a** Dixon plot of inhibition of E186A (prep. 1) catalyzed hydrolysis of 4NPX by TEA at pH 7.0 and 25°C. Reactions containing 51 μM 4NPX and the indicated TEA concentrations were monitored continuously (method A) at 400 nm for 35 min. Curves were drawn from kinetic data fitted to Eq. 3: $v_{enz1} = (1.27 \pm 0.01) \times 10^{-4}\,\mathrm{s}^{-1}$, $v_{enz2} = (3.19 \pm 0.04) \times 10^{-5}\,\mathrm{s}^{-1}$, $K_{i(enz1)}^{TEA} = 0.127 \pm 0.003\,\mathrm{mM}$, and $K_{i(enz2)}^{TEA} = 149 \pm 8\,\mathrm{mM}$. **b** Determination of kinetic parameters for enzyme 2 (prep. 5) at pH 7.0 and 25°C. Reactions containing 0.205–5.12 mM 4NPX and (*filled circle*) 100 mM TEA or (*unfilled square*) 200 mM TEA were monitored continuously (method A) at 400 nm for 35 min. Curves were drawn from the kinetic data fitted to Eq. 2: $k_{cat(enz2)} = (1.86 \pm 0.03) \times 10^{-3}\,\mathrm{s}^{-1}$, $K_{m(enz2)} = 2.72 \pm 0.14\,\mathrm{mM}$, and $K_{i(enz2)}^{TEA} = 121 \pm 9\,\mathrm{mM}$. **c** Determination of kinetic parameters for inhibition of E186A (prep. 5) catalyzed hydrolysis of 4NPX at pH 6.0 and 25°C. Reactions, containing the indicated concentrations of 4NPX and TEA, were monitored continuously at 400 nm (method A) for 20–35 min. Curves were drawn from the kinetic data fitted to Eq. 4: $k_{cat(enz1)} = 0.0272 \pm 0.0003\,\mathrm{s}^{-1}$, $k_{cat(enz2)} = 0.00174 \pm 0.00021\,\mathrm{s}^{-1}$, $k_{cat}/K_{m(enz1)} = 0.0128 \pm 0.0002\,\mathrm{s}^{-1}\,\mathrm{mM}^{-1}$, $k_{cat}/K_{m(enz2)} = (6.01 \pm 0.8) \times 10^{-4}\,\mathrm{s}^{-1}\,\mathrm{mM}^{-1}$, $K_{m(enz1)} = 2.12 \pm 0.05\,\mathrm{mM}$, $K_{m(enz2)} = 2.90 \pm 0.58\,\mathrm{mM}$, $K_{i(enz1)} = 0.656 \pm 0.016\,\mathrm{mM}$, $K_{i(enz2)} = 239 \pm 103\,\mathrm{mM}$. **d** Secondary plot of v_{enz1} and v_{enz2} values (obtained from fitting to Eq. 3, the individual curves of **c**) versus [4NPX]. Curves were drawn from fitting data to Eq. 1: $k_{cat(enz1)} = (2.70 \pm 0.07) \times 10^{-2}\,\mathrm{s}^{-1}$, $k_{cat(enz2)} = (1.97 \pm 0.38) \times 10^{-3}\,\mathrm{s}^{-1}$, $k_{cat}/K_{m(enz1)} = (1.29 \pm 0.04) \times 10^{-2}\,\mathrm{s}^{-1}\,\mathrm{mM}^{-1}$, $k_{cat}/K_{m(enz2)} = (5.35 \pm 0.97) \times 10^{-4}\,\mathrm{s}^{-1}\,\mathrm{mM}^{-1}$, $K_{m(enz1)} = 2.10 \pm 0.11\,\mathrm{mM}$, $K_{m(enz2)} = 3.69 \pm 1.33\,\mathrm{mM}$. **e** Secondary plot of $1/K_{i(enz1)app}$ and $1/K_{i(enz2)app}$ values (obtained from fitting to Eq. 3, the individual curves of **c**) versus [4NPX]. Curves were drawn from fitting data to Eq. 5: $K_{m(enz1)} = 2.28 \pm 0.12\,\mathrm{mM}$, $K_{m(enz2)} = 9.03 \pm 11.36\,\mathrm{mM}$, $K_{i(enz1)} = 0.683 \pm 0.016\,\mathrm{mM}$, $K_{i(enz2)} = 357 \pm 96\,\mathrm{mM}$

enzyme 1 from enzyme 2 activities. Therefore, the determined kinetic parameters of enzyme 2 (the E186A variant of SXA) are valid.

pH dependence of kinetic parameters and $1/K_i^{TEA}$ for enzymes 1 and 2 components of E186A preparations are shown in Fig. 2. $1/K_i^{TEA}$ values for enzyme 1 (wild-type-like enzyme) are fitted to Eq. 9, which describes a limit with a pK_a 6.9±0.2 for enzyme on the acidic side and pK_a 8.8±0.3 for inhibitor on the basic side. These values are similar to those determined for wild-type SXA [16]: p$K_{a(enz)}$ of 6.8 assigned to ionization of E186 and pK_a 8.5 assigned to protonation of triethanolamine; the cationic triethanolamine binds to enzyme with the anionic γ carboxylate of E186. The pK_a of TEA is 8.0 in water of ionic strength, I=0.3 M [16]. It is considered that the anionic subsite −1 of the D14⁻E186⁻ SXA raises the pK_a of inhibitor amino group binding to the enzyme over that of the amino group in water [16]. The pH dependence of triethanolamine binding to enzyme 2 of E186A preparations opposes that of enzyme 1. The $1/K_i^{TEA}$ values for enzyme 2 fit well to Eq. 6, which describes a limit with a pK_a of 7.7±0.1 on the acidic side. The pK_a of 6.8 for the wild-type enzyme is lost by replacing E186 with alanine. The pK_a of 7.7 on the acidic side is attributed to the binding of neutral triethanolamine (and not the cationic form of TEA) to the E186A active site; the lower pK_a^{TEA} 7.7 in the E186A active site than the pK_a^{TEA} 8.0 in aqueous solution likely reflects the more lipophilic environment of the E186A active site that favors binding of the neutral TEA over the cationic form of TEA. Importantly, the loss of the carboxyl group of E186 (replacement with alanine) and its associated pK_a of 6.8 is accompanied by an inverted preference (relative to wild-type SXA) for the neutral TEA over the cationic TEA in addition to the loss of the pK_a 6.8.

Because of the consistencies of enzyme 2 content (>99%) and inconsistencies of enzyme 1 content (0.03% to 0.2%) of E186A preparations, pK_a values for kinetic parameters could be determined using several E186A preparations for enzyme 2, but not enzyme 1. The pH dependence of k_{cat} and k_{cat}/K_m for wild-type SXA acting on 4NPX, using values determined from several studies [4, 11, 12, 14, 16], are fitted to Eq. 7, which describes a single limit controlled by a pK_a on the acidic and basic side: 3.5 and 6.8 for k_{cat}^{4NPX} and 4.9 and 7.3 for k_{cat}/K_m^{4NPX} (Fig. 2c). D14⁻E186^H SXA is the active form of enzyme: the pK_a on the acidic side is ascribed to protonation of D14, the catalytic base. The pK_a on the basic side is

Table 1 Kinetic and binding parameters of E186A preparations and wild-type SXA determined at 25°C.

pH substrate preparation no. parameter	Enzyme 1	Enzyme 2	wt-SXA
pH 6.0 4NPA prep. 7			
$k_{cat}^{4NPA}(s^{-1})$	$(7.93\pm0.25)\times10^{-5}$	$(4.48\pm0.11)\times10^{-6}$	3.13 ± 0.02
$k_{cat}/K_m^{4NPA}(s^{-1}\,mM^{-1})$	$(1.67\pm0.09)\times10^{-4}$	$(2.53\pm0.10)\times10^{-5}$	4.38 ± 0.07
$K_m^{4NPA}(mM)$	0.474 ± 0.036	0.177 ± 0.010	0.715 ± 0.015
$K_{i(TEA)}^{4NPA}(mM)$	0.619 ± 0.039	10^{23}	ND
pH 6.0 4NPX prep. 7			
$k_{cat}^{4NPX}(s^{-1})$	$(4.51\pm0.07)\times10^{-3}$	$(1.44\pm0.03)\times10^{-3}$	29.3 ± 0.04
$k_{cat}/K_m^{4NPX}(s^{-1}\,mM^{-1})$	$(1.43\pm0.03)\times10^{-3}$	$(5.10\pm0.15)\times10^{-4}$	48.9 ± 1.0
$K_m^{4NPX}(mM)$	3.15 ± 0.11	2.82 ± 0.12	0.599 ± 0.011
$K_{i(TEA)}^{4NPX}(mM)$	0.592 ± 0.018	418 ± 58	0.541 ± 0.026
pH 6.0 4NPX/4NPA prep. 7			
$k_{cat}^{4NPX}/k_{cat}^{4NPA}(rel)$	56.9 ± 2.0	321 ± 11	9.37 ± 0.06
$k_{cat}/K_m^{4NPX}/k_{cat}/K_m^{4NPA}(rel)$	8.56 ± 0.51	20.1 ± 1.0	11.2 ± 0.3
$(K_m^{4NPX})/(K_m^{4NPA})(rel)$	6.65 ± 0.55	15.9 ± 1.1	0.837 ± 0.023
$K_{i(TEA)}^{4NPX}/K_{i(TEA)}^{4NPA}(rel)$	0.956 ± 0.067	NA	NA
pH 7.0 4NPA prep. 8			
$k_{cat}^{4NPA}(s^{-1})$	$(4.06\pm0.06)\times10^{-5}$	$(3.61\pm0.13)\times10^{-6}$	3.28 ± 0.03
$k_{cat}/K_m^{4NPA}(s^{-1}\,mM^{-1})$	$(3.27\pm0.09)\times10^{-5}$	$(2.37\pm0.50)\times10^{-5}$	3.03 ± 0.04
$K_m^{4NPA}(mM)$	1.24 ± 0.05	0.152 ± 0.036	1.08 ± 0.02
$K_{i(TEA)}^{4NPA}(mM)$	0.141 ± 0.005	$815\pm2,684$	0.121 ± 0.003
pH 7.0 4NPX prep. 8			
$k_{cat}^{4NPX}(s^{-1})$	$(1.47\pm0.05)\times10^{-4}$	$(1.64\pm0.01)\times10^{-3}$	14.4 ± 0.4
$k_{cat}/K_m^{4NPX}(s^{-1}\,mM^{-1})$	$(3.35\pm0.36)\times10^{-4}$	$(5.03\pm0.03)\times10^{-4}$	36.4 ± 1.9
$K_m^{4NPX}(mM)$	0.439 ± 0.058	3.27 ± 0.03	0.394 ± 0.031
$K_{i(TEA)}^{4NPX}(mM)$	0.0955 ± 0.0127	145 ± 3	0.111 ± 0.002
pH 7.0 4NPX/4NPA prep. 8			
$k_{cat}^{4NPX}/k_{cat}^{4NPA}(rel)$	3.63 ± 0.14	456 ± 17	4.38 ± 0.12
$k_{cat}/K_m^{4NPX}/k_{cat}/K_m^{4NPA}(rel)$	10.3 ± 1.1	21.2 ± 4.5	12.0 ± 0.7
$K_m^{4NPX}/K_m^{4NPA}(rel)$	0.354 ± 0.049	21.5 ± 5.1	0.364 ± 0.030
$K_{i(TEA)}^{4NPX}/K_{i(TEA)}^{4NPA}(rel)$	0.677 ± 0.093	0.178 ± 0.586	0.917 ± 0.028
pH 8.0 4NPA prep. 7			
$k_{cat}^{4NPA}(s^{-1})$	$(9.16\pm0.17)\times10^{-5}$	$(4.39\pm0.14)\times10^{-6}$	3.05 ± 0.02
$k_{cat}/K_m^{4NPA}(s^{-1}\,mM^{-1})$	$(2.67\pm0.05)\times10^{-5}$	$(3.29\pm0.48)\times10^{-5}$	0.746 ± 0.005
$K_m^{4NPA}(mM)$	3.43 ± 0.12	0.133 ± 0.021	4.09 ± 0.05
$K_{i(TEA)}^{4NPA}(mM)$	0.122 ± 0.003	47.0 ± 16.5	ND
pH 8.0 4NPX prep. 7			
$k_{cat}^{4NPX}(s^{-1})$	$(1.57\pm0.11)\times10^{-3}$	$(1.60\pm0.02)\times10^{-3}$	2.36 ± 0.01
$k_{cat}/K_m^{4NPX}(s^{-1}\,mM^{-1})$	$(1.98\pm0.08)\times10^{-4}$	$(6.23\pm0.07)\times10^{-4}$	7.13 ± 0.11
$K_m^{4NPX}(mM)$	7.93 ± 0.86	2.57 ± 0.05	0.331 ± 0.006
$K_{i(TEA)}^{4NPX}(mM)$	0.100 ± 0.008	33.2 ± 0.8	$(8.80\pm0.22)\times10^{-2}$
pH 8.0 4NPX/4NPA prep. 7			
$k_{cat}^{4NPX}/k_{cat}^{4NPA}(rel)$	17.1 ± 1.3	365 ± 12	0.772 ± 0.007
$k_{cat}/K_m^{4NPX}/k_{cat}/K_m^{4NPA}(rel)$	7.40 ± 0.33	18.9 ± 2.8	9.55 ± 0.15

Table 1 (continued).

pH substrate preparation no. parameter	Enzyme 1	Enzyme 2	wt-SXA
$\left(K_m^{4NPX}\right)/\left(K_m^{4NPA}\right)$ (rel)	2.31 ± 0.26	19.3 ± 3.1	$(8.08\pm0.18)\times10^{-2}$
$K_{i(TEA)}^{4NPX}/K_{i(TEA)}^{4NPA}$ (rel)	0.893 ± 0.075	0.706 ± 0.249	NA

Parameters of enzyme 1 and enzyme 2 in E186A preparations were determined by varying substrate (4NPX and 4NPA) and triethanolamine concentrations in reactions at 25°C and the indicated pH. Initial rate data were fitted globally to Eq. 4. Standard errors are indicated. Wild-type SXA parameters are combined values of those published previously [4, 11] and unpublished values determined from fitting data for K_i determinations [12, 14, 16]

ND not determined, NA not applicable

ascribed to ionization of the catalytic acid (E186). With the E186A mutant (enzyme 2), the pH dependencies could not be studied below pH 6.0, owing to denaturation of protein interfering with spectroscopic measurements. The E186A mutant loses the pK_a ~7, assigned to E186, and the pH dependence of k_{cat}^{4NPX} and k_{cat}/K_m^{4NPX} become nearly pH independent, with the small dependence described by lines of small slopes (Fig. 2c). $1/K_m^{4NPX}$ for wild-type SXA has two limits and two pK_a's for its pH dependence described by Eq. 8 (Fig. 2d). pK_a 5 is assigned to the ionization of D14 to form the catalytically active D14$^-$E186^H enzyme form. pK_a 7 is assigned to ionization of E186 to form D14$^-$E186$^-$. Thus, the wild-type SXA, in its catalytically inactive dianionic enzyme form, D14$^-$E186$^-$, has greater affinity than the catalytically active form, D14$^-$E186^H for substrate 4NPX. It is notable that 4NPA binds only to the catalytically active form, D14$^-$E186^H, and the pH profile of $1/K_m^{4NPA}$ is unlike that of $1/K_m^{4NPX}$ and more like the bell-shaped dependencies of k_{cat}/K_m^{4NPA} and k_{cat}/K_m^{4NPX} [4]. E186A has little pH dependence for binding 4NPX and its pH profile for $1/K_m^{4NPX}$ is described by a line with small slope (Fig. 2d).

Kinetic parameters for substrates, 4NPX and 4NPA, and K_i^{TEA} values were determined for enzymes 1 and 2 components of E186A preparations at constant ionic strength ($I=$ 0.3 M), 25°C, and pH 6.0, 7.0, and 8.0 by fitting the kinetic data globally to Eq. 4 (Table 1). Initial rate data for 4NPX and 4NPA were determined using the same E186A preparations so that ratios of kinetic parameters, can be appropriately calculated, even for those determined for enzyme 1, which varies from preparation to preparation with respect to k_{cat}^{4NPX}. Kinetic parameters for enzyme 2 acting on one substrate by one E186A preparation can be used for comparing with kinetic parameters for enzyme 2 acting on another substrate by another E186A preparation as can be seen by comparing values and relative values (4NPX/4NPA) in Table 1 (same E186A preparations for both substrates) and Table 2 (different E186A preparations for 4NPX and 4NPA). The most outstanding determination listed in Tables 1 and 2 is the change in the relative parameter $k_{cat}^{4NPX}/k_{cat}^{4NPA}$ of E186A (enzyme 2) in comparison to that of wt-SXA, which occurs at all three of the pH values examined. At pH 6.0, 7.0, and 8.0, the respective $k_{cat}^{4NPX}/k_{cat}^{4NPA}$ values are 321, 456, and 365 for E186A (enzyme 2), and the respective values for wt-SXA are 9.37, 4.38, and 0.77. Also, $k_{cat}^{4NPX}/k_{cat}^{4NPA}$ values of 389 at pH 6.0 and 427 at pH 7.0 for E186A (enzyme 2), shown in Table 2 and calculated from initial rate data of different E186A preparations, are similar to those in Table 1. Relative substrate specificity values, $k_{cat}/K_m^{4NPX}/k_{cat}/K_m^{4NPA}$, of E186A (enzyme 2; 20.1, 21.2, and 18.9, respectively, at pH 6.0, 7.0, and 8.0) are twofold those of the wt-SXA, but considerably lower than the $k_{cat}^{4NPX}/k_{cat}^{4NPA}$ values of E186A (enzyme 2). The latter is due to the lower values of K_m^{4NPA} compared to those of K_m^{4NPX} held by E186A (enzyme 2) at each pH. In addition and at each pH, the K_m^{4NPA} values held by

⁂ Humana Press
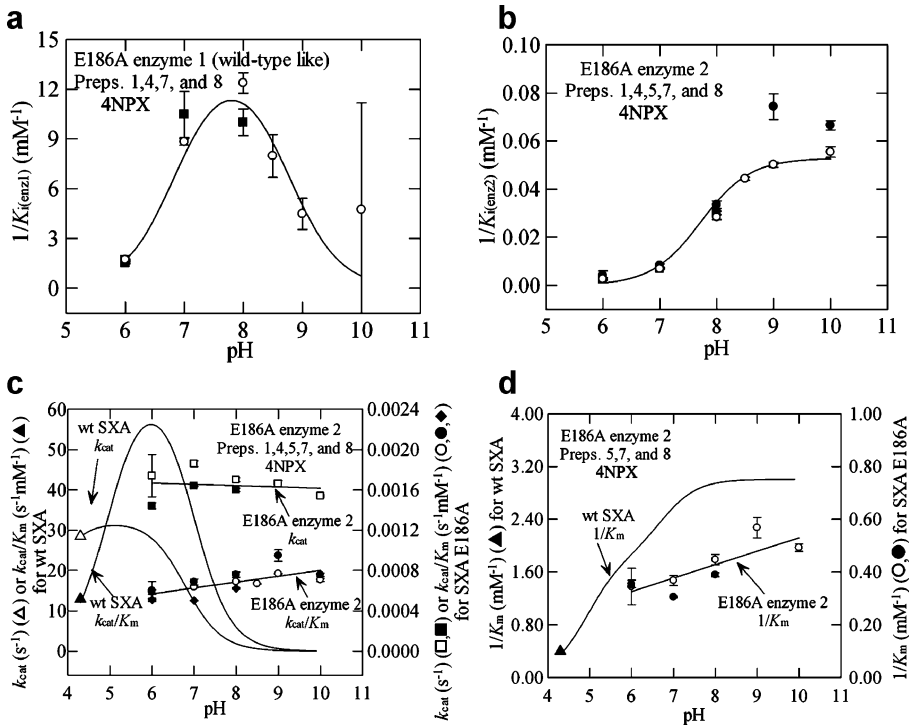
Fig. 2 Influence of pH on kinetic parameters determined for β-xylosidase components of E186A SXA preparations acting on 4NPX at 25°C. **a** Influence of pH on $1/K_{i(enz1)}^{TEA}$ (wild-type-like SXA affinity) at 25°C. $1/K_{i(enz1)}$ values were determined by methods illustrated by Fig. 1a, c. The curve was drawn from $1/K_{i(enz1)}$ values fitted to Eq. 9 (two pK_a's): pH-independent $1/K_{i(enz1)}^{TEA} = 14.1 \pm 4.3$ mM^{-1}, $pK_{a(enz1)} = 6.9 \pm 0.2$ and $pK_{a(inh)} = 8.8 \pm 0.3$. **b** Influence of pH on $1/K_{i(enz2)}$ for TEA (weak binding affinity) at 25°C. $K_{i(enz2)}$ values were determined by the methods shown in Fig. 1a (*unfilled circle*), b (*filled circle*), and c (*filled square*). $1/K_{i(enz2)}$ values were fitted to Eq. 6 (single pK_a): pH-independent $1/K_{i(enz2)} = 0.0529 \pm 0.0091$ mM^{-1} and $pK_a = 7.7 \pm 0.1$. **c** Comparison of influence of pH on k_{cat} and k_{cat}/K_m of wild-type SXA and E186A SXA acting on 4NPX at 25°C. Wild-type SXA values for k_{cat} and k_{cat}/K_m are combined values of those published previously [4, 11] and unpublished values determined from fitting data for K_i determinations [12, 14, 16]. Fitted parameters for wild-type SXA k_{cat} (*unfilled triangle*) from fits to Eq. 7: pH-independent $k_{cat} = 32.5 \pm 0.4$ s^{-1}, $pK_{a1} = 3.5 \pm 0.1$ and $pK_{a2} = 6.8 \pm 0.01$. Fitted parameters for wild-type SXA k_{cat}/K_m (*filled triangle*) from fit to Eq. 7: pH-independent $k_{cat}/K_m = 67.1 \pm 1.2$ mM^{-1} s^{-1}, $pK_{a1} = 5.0 \pm 0.03$ and $pK_{a2} = 7.0 \pm 0.02$. k_{cat} (*unfilled square, filled square*) values of E186A SXA were determined from the experiments described in Fig. 1b (*unfilled square*) and c (*filled square*). k_{cat}/K_m values of E186A SXA were determined from the experiments described in Fig. 1a (*unfilled circle*), b (*filled circle*), and c (*filled diamond*). Values at varying pH were fitted to lines for k_{cat}(slope $= -(1.28 \pm 3.66) \times 10^{-5}$ and intercept $= (1.75 \pm 0.28) \times 10^{-3}$) and k_{cat}/K_m(slope $= (5.81 \pm 1.72) \times 10^{-5}$ and intercept $= (2.20 \pm 1.37) \times 10^{-4}$). **d** Comparison of influence of pH on $1/K_m$ of wild-type SXA and E186A SXA acting on 4NPX at 25°C. Wild-type SXA values for $1/K_m$ are combined values of those published previously [4, 11] and unpublished values determined from fitting data for K_i determinations [12, 14, 16]. Fitted parameters for wild-type SXA $1/K_m$ (*filled triangle*) fitted to Eq. 8: middle limit of $1/K_m = 2.04 \pm 0.06$ mM^{-1}, upper limit of $1/K_m = 2.99 \pm 0.03$, $pK_{a1} = 4.9 \pm 0.02$ and $pK_{a2} = 6.7 \pm 0.1$. $1/K_m$ values of E186A were determined from the experiments described in Fig. 1b (*unfilled circle*) and c (*filled circle*). $1/K_m$ values versus pH were fitted to a line: slope $= 0.0510 \pm 0.0145$ and intercept $= 0.0201 \pm 0.112$

E186A (enzyme 2) are considerably lower than those of wt-SXA and the K_m^{4NPX} values held by E186A (enzyme 2) are considerably higher than those of wt-SXA. Thus, 4NPA is substantially worse than 4NPX as substrate for E186A (enzyme 2) than the case with wt-SXA. Steady-state catalysis is little affected by diffusion as shown by the similar kinetic

Table 2 Relative parameters of enzyme 2 acting on 4NPX and 4NPA obtained by using values from two different preparations.

pH substrate preparation no. parameter	Enzyme 2
pH 6.0 4NPX prep. 6	
$k_{cat}^{4NPX} (s^{-1})$	$(1.74 \pm 0.21) \times 10^{-3}$
$k_{cat}/K_m^{4NPX} (s^{-1}\, mM^{-1})$	$(6.01 \pm 0.86) \times 10^{-4}$
$K_m^{4NPX} (mM)$	2.90 ± 0.58
$K_{i(TEA)}^{4NPX} (mM)$	239 ± 103
pH 6.0 4NPX/4NPA prep. 6/7	
$k_{cat}^{4NPX}/k_{cat}^{4NPA} (rel)$	389 ± 47
$k_{cat}/K_m^{4NPX}/k_{cat}/K_m^{4NPA} (rel)$	23.7 ± 3.5
$(K_m^{4NPX})/(K_m^{4NPA}) (rel)$	16.4 ± 3.4
$K_{i(TEA)}^{4NPX}/K_{i(TEA)}^{4NPA} (rel)$	NA
pH 7.0 4NPX prep. 7	
$k_{cat}^{4NPX} (s^{-1})$	$(1.54 \pm 0.02) \times 10^{-3}$
$k_{cat}/K_m^{4NPX} (s^{-1}\, mM^{-1})$	$(5.96 \pm 0.10) \times 10^{-4}$
$K_m^{4NPX} (mM)$	2.59 ± 0.07
$K_{i(TEA)}^{4NPX} (mM)$	136 ± 9
pH 7.0 4NPX/4NPA prep. 7/8	
$k_{cat}^{4NPX}/k_{cat}^{4NPA} (rel)$	427 ± 17
$k_{cat}/K_m^{4NPX}/k_{cat}/K_m^{4NPA} (rel)$	25.1 ± 5.3
$K_m^{4NPX}/K_m^{4NPA} (rel)$	17.0 ± 4.1
$K_{i(TEA)}^{4NPX}/K_{i(TEA)}^{4NPA} (rel)$	0.167 ± 0.549

Parameters of E186A enzyme 2 acting on 4NPX were determined at 25°C and the indicated pH by the methods illustrated by Fig. 1c (data fitted to Eq. 4 globally). Parameters for enzyme 2 of prep. 7 acting on 4NPA at pH 6.0 and enzyme 2 of prep. 8 acting on 4NPA at pH 7.0 are listed in Table 1. Standard errors are indicated

NA not applicable

parameters obtained for SXA acting on substrates, 4NPX and 4NPA, in media that varied sixfold in relative viscosity and neither bursts nor lags are seen in the pre-steady-state progress curves of SXA acting on 4NPX and 4NPA [4]. Therefore, K_m values approximate thermodynamic equilibrium dissociation constants, and k_{cat} values approximate rates of the glycoside hydrolysis step on the enzyme.

Wild-type-like enzyme 1 has similar K_i^{TEA} and K_m^{4NPA} values as wt-SXA at pH 6.0, 7.0, and 8.0 (Table 1). Its K_m^{4NPX} value is similar at pH 7.0 (Table 1), but at pH 6.0 and 8.0, K_m^{4NPX} values for enzyme 1 are much larger than those of wt-SXA. Kinetic constants at pH 7.0, including K_m^{4NPX}, were determined using preparation 8, which happens to have one of the lowest enzyme 1 activities among the preparations studied. Preparation 7 was used for determination of kinetic constants at pH 6.0 and 8.0, and the preparation's activity for enzyme 1 was 22-fold higher than that of preparation 8 enzyme 1. Kinetic constants for enzyme 1 of preparation 7 acting on 4NPX at pH 7.0 and 25°C are K_{cat}^{4NPX} ($0.00330 \pm 0.00007\ s^{-1}$), k_{cat}/K_m^{4NPX} ($0.000894 \pm 0.00002\ s^{-1}\ mM^{-1}$), and K_m^{4NPX} ($3.69 \pm 0.15\ mM$). Thus, it can be seen that, unlike the K_m^{4NPX} determined for preparation 8 enzyme 1 (similar to wt-SXA), enzyme 1 of preparation 7 has a much larger K_m^{4NPX} than wt-SXA at pH 7.0, just as it does at pH 6.0 and 8.0. It is emphasized that we do not know the sequence identity of enzyme 1, but we do know that the protein derives from the E186A gene. It appears that translational misreading accounts for the existence of

enzyme 1, and with this in mind, it seems that greater enzyme 1 activity in a E186A preparation indicates greater translational misreading activity, which could lead to more than one (E186A back to E186) translational misreading event occurring per E186A molecule, changing other alanine residues to glutamates or other amino acids to give rise to the appearance of enzyme 1 with different kinetic properties than wt-SXA, such as high K_m^{4NPX}.

The E186G mutant was prepared to determine whether the glycine substitution has similar influences on kinetic properties of SXA as the E186A mutation. Kinetic parameters and K_i^{TEA} values were determined for enzymes 1 and 2 components of the E186G preparations acting on 4NPX at pH 8.0 and 25°C (Fig. 3). Parameters were determined by fitting the initial-rate data globally to Eq. 4. Values for $k_{cat}^{4NPX}(6.00 \pm 0.21) \times 10^{-4} \, s^{-1}$ and $k_{cat}/K_m^{4NPX}(2.76 \pm 0.18) \times 10^{-4} \, s^{-1} \, mM^{-1}$, determined for enzyme 2 of the E186G preparation, are one half those determined for enzyme 2 of the E186A preparation under similar conditions (Table 1). The K_m^{4NPX} value (2.17±0.12 mM) is 16% lower than that of the E186A mutant. The K_i^{TEA} value (11.0±1.1 mM) is one third that of E186A at pH 8.0 (Table 1). It was also determined that the enzyme 2 component of the E186G preparation has much lower activity on 4NPA than 4NPX; it was so low that kinetic parameters could not be accurately determined. Thus, it appears that the E186G mutation confers similar effects to SXA as the E186A mutation.

Previously we reported that at pH 5.3 and 25°C, the E186A mutation retained 0.0086% of k_{cat}^{4NPX} held by wild-type SXA and its K_m^{4NPX} was 40% higher than that of wild-type SXA [4]. Relative parameters, $k_{cat}^{4NPX}/k_{cat}^{4NPA}$ and $k_{cat}/K_m^{4NPX}/k_{cat}/K_m^{4NPA}$ were listed as 11.2 and 13.4, respectively, for E186A and as 11.6 and 12.3, respectively, for the wild-type enzyme. From the resolution of kinetic parameters made possible by titrating out the wild-type-like component (enzyme 1) of the E186A preparations with triethanolamine, it was determined here that the E186A SXA retains 0.0049% (pH 6.0), 0.011% (pH 7.0), and 0.068% (pH 8.0) of k_{cat}^{4NPX} held by wild-type SXA at the same pH. $k_{cat}^{4NPX}/k_{cat}^{4NPA}$ values of the E186A mutant are 34-fold (pH 6.0), 100-fold (pH 7.0), and 470-fold (pH 8.0) those of wt-SXA at the same pH (Table 1). $k_{cat}/K_m^{4NPX}/k_{cat}/K_m^{4NPA}$ values of E186A are 20-fold those of wt-SXA at each pH. Clearly, the major correction made in this work is not that of absolute rates of the
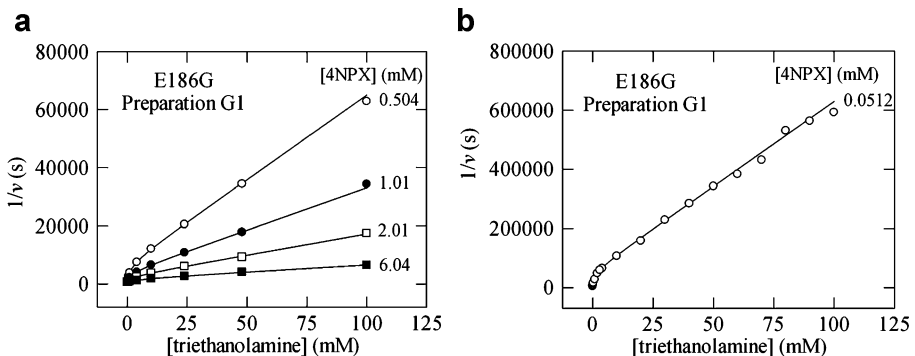
Fig. 3 Influence of triethanolamine on kinetic parameters of E186G SXA (prep. G1) at pH 8.0 and 25°C. **a** Reactions containing the indicated concentrations of 4NPX and TEA were monitored discontinuously at 400 nm (method B) for 44–156 min. **b** Reactions containing the indicated concentrations of 4NPX and TEA were monitored continuously at 400 nm (method A) for 20–240 min. Curves were drawn from the kinetic data of **a**, **b** fitted globally to Eq. 4: $k_{cat(enz1)} = (1.26 \pm 0.02) \times 10^{-3} \, s^{-1}$, $k_{cat(enz2)} = (6.00 \pm 0.21) \times 10^{-4} \, s^{-1}$, $k_{cat}/K_{m(enz1)} = (3.88 \pm 0.10) \times 10^{-3} \, s^{-1} \, mM^{-1}$, $k_{cat}/K_{m(enz2)} = (2.76 \pm 0.18) \times 10^{-4} \, s^{-1} \, mM^{-1}$, $K_{m(enz1)} = 0.325 \pm 0.011 \, mM$, $K_{m(enz2)} = 2.17 \pm 0.12 \, mM$, $K_{i(enz1)} = 0.0962 \pm 0.0044 \, mM$, $K_{i(enz2)} = 11.0 \pm 1.1 \, mM$

E186A mutant. Instead, it resides in the relative kinetic parameters of E186A acting on 4NPX and 4NPA. The relative k_{cat} values of E186A acting on 4NPX and 4NPA show that the mutation more severely damages activity on 4NPA than 4NPX. This result is in accord with the idea that enzyme acting on 4NPX must deal more with glycone ring distortion than the enzyme acting on 4NPA; this has been borne out by certain mutations of subsite −1 residues, whose mutant enzymes exhibit lower $k_{cat}^{4NPX}/k_{cat}^{4NPA}$ values than wild-type SXA [11]. The $k_{cat}^{4NPX}/k_{cat}^{4NPA}$ values of E186A are higher than those of wild-type SXA, supporting the idea that E186, in its role as catalytic acid, is more important for transition state stabilization of the 4NPA reaction than the 4NPX reaction.

Aminoalcohols are effective tools for probing active sites of glycoside hydrolases, as shown here, where aminoalcohols have been useful in differentiating binding to subsites −1 and +1 of SXA and resolving the activity of E186A from that of a wild-type-like contaminant. In combination with site-directed mutagenesis, substrates with different physical properties, relevant to the reaction coordinate, are generally useful in pinpointing roles of native amino acid residues in stabilizing different aspects of the reaction's transition state. This strategy was first applied to identify active-site residues involved in distorting substrate ring conformations to their transition-state geometries mandated by stereo-electronic principles in the case of scytalone dehydratase acting on scytalone and the more easily deformed alternate substrate 2,3-dihydro-2,5-dihydroxy-4H-benzopyran-4-one [21]. The strategy was first applied to glycoside hydrolases in the case of SXA acting on 4NPX and 4NPA [11]. The energy barrier for conformational inversion of pyranoses (10 kcal/mol) is considerably higher than that of furanoses (3–4 kcal/mol) [17], and distortion of pyranoside substrates from the ground-state chair conformation is well recognized as a major task for the catalyst [22–30]. SXA active-site residues R290 and F31, important for promoting both 4NPA and 4NPX reactions, were identified as being more important for the SXA-catalyzed hydrolysis of 4NPX than that of 4NPA, strongly suggesting involvement of the two residues in promoting conformational inversion. In the current work, the strategy was reversed by selecting an active-site residue, E186, which was considered unlikely to have a role in substrate distortion owing to its distance from the glycone ring of substrate and its assigned role as catalytic acid. It was viewed that the single transition state of SXA-catalyzed reactions can be divided into two components: factors that support ring distortion and factors that support other aspects of the hydrolysis reaction (i.e., protonation, C1 migration, and activation of the nucleophilic water). Our demonstration that the E186A mutation severely decreases activity on both substrates, but is much more deleterious to the enzyme acting on 4NPA than 4NPX, validates this view.

References

1. Henrissat, B. (1991). *Biochemical Journal, 280*, 309–316.
2. Henrissat, B., & Davies, G. J. (1997). *Current Opinion in Structural Biology, 7*, 637–644.
3. Davies, G. J., & Sinnott, M. L. (2008). *The Biochemical Journal.* www.biochemj.org. doi:10.1042/BJ20080382.
4. Jordan, D. B., Li, X.-L., Dunlap, C. A., Whitehead, T. R., & Cotta, M. A. (2007). *Applied Biochemistry and Biotechnology, 141*, 51–76.
5. Jordan, D. B. (2008). *Applied Biochemistry and Biotechnology, 146*, 137–149.
6. Jordan, D. B., Li, X.-L., Dunlap, C. A., Whitehead, T. R., & Cotta, M. A. (2007). *Applied Biochemistry and Biotechnology, 137–140*, 93–104.
7. Jordan, D. B., Dien, B. S., Li, X.-L., & Cotta, M. A. (2006). In Renewable Energy 2006 Committee (Ed.), *Proceedings of Renewable Energy 2006* (pp. 1036–1041). Japan: Makuhari Messe.

8. Saha, B. C. (2003). *Journal of Industrial Microbiology & Biotechnology, 30*, 279–291.
9. Gray, K. A., Zhao, L., & Emptage, M. (2006). *Current Opinion in Chemical Biology, 10*, 141–146.
10. Shallom, D., & Shoham, Y. (2003). *Current Opinion in Microbiology, 6*, 219–228.
11. Jordan, D. B., & Li, X.-L. (2007). *Biochimica et Biophysica Acta, 1774*, 1192–1198.
12. Jordan, D. B., & Braker, J. D. (2007). *Archives of Biochemistry and Biophysics, 465*, 231–246.
13. Whitehead, T. R., & Cotta, M. A. (2001). *Current Microbiology, 43*, 293–298.
14. Brunzelle, J. S., Jordan, D. B., McCaslin, D. R., Olczak, A., & Wawrzak, Z. (2008). *Archives of Biochemistry and Biophysics, 474*, 157–166.
15. Jordan, D. B., & Braker, J. D. (2009). *Applied Biochemistry and Biotechnology, 155*, 330–346.
16. Jordan, D. B., Mertens, J. A., & Braker, J. D. (2009). *Biochimica et Biophysica Acta, 1794*, 144–158.
17. Durette, P. L., & Horton, D. (1971). *Advances in Carbohydrate Chemistry and Biochemistry, 26*, 49–125.
18. Kezdy, F. J., & Bender, M. L. (1962). *Biochemistry, 1*, 1097–1106.
19. Gill, S. C., & von Hippel, P. H. (1989). *Analytical Biochemistry, 182*, 319–326.
20. Leatherbarrow, R. J. (2001). *Grafit Version 5*. Horley: Erithacus Software Ltd.
21. Zheng, Y.-J., Basarab, G. S., & Jordan, D. B. (2002). *Biochemistry, 41*, 820–826.
22. Sulzenbacher, G., Driguez, H., Henrissat, B., Scülein, M., & Davies, G. J. (1996). *Biochemistry, 35*, 15280–15287.
23. Tews, I., Perrakis, A., Oppenheim, A., Dauter, Z., Wilson, K. S., & Vorgias, C. E. (1996). *Nature Structural & Molecular Biology, 3*, 638–648.
24. Davies, G. J., Mackenzie, L., Varrot, A., Dauter, M., Brzozowski, A. M., Scülein, M., et al. (1998). *Biochemistry, 37*, 11707–11713.
25. Notenboom, V., Birsan, C., Nitz, M., Rose, D. R., Warren, R. A., & Withers, S. G. (1998). *Nature Structural & Molecular Biology, 5*, 812–818.
26. Sidhu, G., Withers, S. G., Nguyen, N. T., McIntosh, L. P., Ziser, L., & Brayer, G. D. (1999). *Biochemistry, 38*, 5346–5354.
27. Vocadlo, D. J., Davies, G. J., Laine, R., & Withers, S. G. (2001). *Nature, 412*, 835–838.
28. Ducros, V. M.-A., Zechel, D. L., Murshudov, G. N., Gilbert, H. J., Szabó, L., Stoll, D., et al. (2002). *Angewandte Chemie. International Edition, 41*, 2824–2827.
29. Larsson, A. M., Bergfors, T., Dultz, E., Irwin, D. C., Roos, A., Driguez, H., et al. (2005). *Biochemistry, 44*, 12915–12922.
30. Biarnés, X., Nieto, J., Planas, A., & Rovira, C. (2006). *Journal of Biological Chemistry, 281*, 1432–1441.